Published by
NIGERIAN SOCIETY OF PHYSICAL SCIENCES
Available online @ https://asr.nsps.org.ng/index.php/asr

African Scientific Reports 4 (2025) 328

African Scientific Reports

Measurement and simulation of indoor radon concentration distribution in students' residential hostels around Ladoke Akintola University of Technology, Ogbomoso, Nigeria

E. A. Oni[a], C. O. Ajiboye[a,*], P. S. Ayanlola[a], O. O. Oloyede[a], A. A. Aremu[a], T. A. Olajide[a], O. O. Oladapo[b], O. P. Oyero[c], A. E. Oladipo[d], M. K. Lawal[b]

[a] *Department of Pure and Applied Physics, Ladoke Akintola University of Technology, Ogbomoso, Nigeria*
[b] *Department of Science Laboratory Technology, Ladoke Akintola University of Technology, Ogbomoso, Nigeria*
[c] *Department of Physics, Adeleke University Ede, Nigeria*
[d] *Department of Physics, Bowen University Iwo, Osun State, Nigeria*

Abstract

Radon is a harmful gas and class I carcinogen posing global challenge to human health. Being an inert gas, it is impossible to perceive its presence by any of the sense organs, thus the application of Computational Fluid Dynamics (CFD) simulation in radon study is enhancing human understanding of the behavior and distribution of radon in indoor air. Hence, this work measured the indoor radon concentration (R_i) in student's residential hostels and evaluate radon gas distribution in indoor air. In-situ measurement of the R_i in 10 student's residential hostels was carried for a period of one month using RAD7. The CFD code ANSYS Fluent 2024R2, based on the finite volume method was employed in modeling the geometry of the student's room, calculate, predict and visualize the concentration and distribution of radon inside the room. The average measured R_i was 45.89 Bq/m^3 with a corresponding annual effective dose of 1.042 mSv/yr. The simulation revealed an average value of 45.51 Bq/m^3 and the annual effective dose from the inhalation of radon when ACH is 2, 3 and 4 h^{-1}, respectively, was calculated to be 1.03 mSv/yr, which is lower than the recommended value by ICRP. The simulation revealed that radon gas is more concentrated at the building window compare to other parts of the building. It is therefore recommended that the indoor radon induced air be diffused with external or fresh air by ensuring adequate ventilation and maintaining healthy air circulation.

DOI:10.46481/asr.2025.4.3.328

Keywords: Indoor radon, Air change rate, Annual absorbed dose, Annual effective dose, Radon monitoring

Article History :
Received: 02 June 2025
Received in revised form: 15 August 2025
Accepted for publication: 19 August 2025
Published: 07 September 2025

1. Introduction

The environment is crucial for sustaining life on Earth, because it provides the resources that life depends on, like soil, water, and air, the environment is essential to maintaining life on Earth. Although all of these resources are necessary, air and water are particularly essential because human life would not be possible without them [1]. These resources are subject to different levels of contaminations, such as natural and artificial radionuclides, of which radon, a naturally occurring radionuclide, make up the majority

*Corresponding author: Tel. No.: +234-816-954-4249.
Email address: oluwaseunchristianah40@gmail.com (C. O. Ajiboye)

of the total natural background radiation [2]. Radon is a dangerous gas which is the second most prevalent cause of lung cancer in smokers and the most common cause in non-smokers [3, 4]. The health hazards that come with radon gas exposure to humans have attracted a lot of national research interest [5]. In outdoor environment, radon concentrations are not considered as health risk because radon that escapes into the atmosphere usually disperses fast. Nevertheless, radon accumulation indoors raises the concentration of radon activity, which might lead to health issues in the respiratory system [6]. Indoor air quality and ventilation system have a significant impact on the concentration of radon indoors [7]. Despite being a well-established practice, air pollution monitoring is still a useful tool in daily life. It has progressed from conventional techniques to sophisticated computer systems that track air quality, and since everyone needs clean air, a variety of technologies have been put in place to provide real-time air quality data, which has proven to be very successful in creating a healthier environment [8].

Several studies have been carried out both locally and internationally on the measurement of radon concentration in indoor buildings. A study by Ref. [5] reported that the lithology feature on which the buildings investigated in selected study locations of southwestern Nigeria influences the indoor radon concentration. In another study by Ref. [9], it was reported that on the average, there is 0.2% to 0.6% of occurrence of lifetime cancer from chronic exposure to low-level radon gas using both the dosimetric and simulation approach when investigating workplaces of some tertiary institutions in western Nigeria. Recently, computational fluid dynamics (CFD) has emerged as crucial instrument for investigating how radon behaves in indoor air. It is a low-cost technique that can effectively model and forecast air flow patterns, indoor air conditions, and the distribution of pollutants in a space [10]. In applying CFD to three different rooms geometry, Ref. [11] reported that as the volume of the room increases, radon is mitigated more rapidly and therefore lower levels of concentration of this gas. Other several studies have also reported the application of CFD to radon study internationally. However, a thorough search of the exiting literature from Nigeria revealed no work has been done on the application of CFD to radon study, thereby leaving Nigeria behind of the technological advancement. Thus, this study adopts the exiting method of quantifying radon concentration through measurement and applies CFD to simulate it distribution in indoor air. This study will serve as a benchmark for subsequent work on the application of CFD on radon assessment in Nigeria.

2. Methodology

This study was carried out in 10 different students' hostels around Ladoke Akintola University of Technology, Ogbomoso, Nigeria, situated on latitude 8°8'0" North and longitude 4°16′0″ East. The hostels covering areas like Adenike, Under G, YOACO, Stadium, Aroje and Isale general of the university environment were randomly selected covering buildings of 15 years old and new once. Furthermore, the buildings are of the same ventilation and floor level structure, designed with a natural ventilation system that utilizes strategically placed opening like allowing fresh air circulation throughout the interior spaces without mechanical aids.

2.1. Radon measurement

An active radon detector, RAD7, made in U.S by DURRIDGE Company was used for the measurements. When radon is deposited on the detector surface, it instantly emits high-energy alpha particles into the solid-state detector. Electrical signal is formed by the detector and then via electronic circuit this signal is converted to digital form.

2.2. Dose estimation

The annual absorbed dose for each room was estimated using equation (1) and the annual effective dose was estimated using equation (2) [12, 13]:

$$D\left(\frac{\text{mSv}}{\text{y}}\right) = C_{\text{Rn}} D_c F H T, \tag{1}$$

$$E\left(\frac{\text{mSv}}{\text{y}}\right) = D W_R W_T, \tag{2}$$

where C_{Rn} represents the average radon concentrations in the room (Bq/m^3), D_c represent dose conversion factor of radon (9.0×10^{-6} mSv/h per Bq/m^3), F represents the indoor equilibrium factor for radon of 0.4 [14], H is the occupancy factor (0.4) and T is the number of hours spent indoor annually (18 hrs × 365 days). In equation (2), D is the annual absorbed dose (mSv/y); W_T is the tissue weighting factor for the lung (0.12); W_R is the radiation weighting factor for alpha particles (20) [12, 13].

2.3. Numerical method

The simulation was conducted using computational fluid dynamics, which offers numerical approximations to the equations governing fluid motion. Three steps must be taken before applying CFD to analyze a fluid problem: first, the mathematical equations describing the fluid flow, which are typically a collection of partial differential equations. The domain was then separated into tiny grids or elements after these equations were discretized to create a numerical counterpart. Ultimately, these equations were solved using the initial conditions and the boundary conditions iteratively and certain control parameters are used to control the convergence, stability, and accuracy of the method.

2.3.1. Governing equations

The equations governing the fluid flow could be expressed as follows [15, 16].

(a) Conservation of mass

For 3 dimensional incompressible and steady flow, it is written by equation (3) as:

$$\nabla \cdot \mathbf{v} = 0, \tag{3}$$

that is, the velocity of the fluid is such that the rate of volume flow into any region of the 3-dimensional space is equal to the rate of volume flow out, and $\mathbf{v}$ is the velocity vector of the fluid.

(b) Conservation of momentum

For 3 dimensional incompressible and steady flow, it is written by equation (4) as

$$\rho(\mathbf{v} \cdot \nabla \mathbf{v}) = -\nabla p + \mu \nabla^2 \mathbf{v} + \mathbf{f}, \tag{4}$$

where $\mathbf{v}$ represent the velocity vector of the fluid (v_x, v_y, v_z), ρ represent the fluid density, p is pressure of the fluid, $\mathbf{v} \cdot \nabla \mathbf{v}$ is the advection (convection) of momentum where the velocity of the fluid at each point carries momentum, $\mu \nabla^2 \mathbf{v}$ is the viscous force (internal friction due to the fluid's viscosity), $-\nabla p$ is pressure gradient force (change in pressure), $\mathbf{f}$ is the external or body force (gravitational or electromagnetic).

(c) Conservation of energy

For 3 dimensional incompressible and steady flow, it is written by equation (5) as

$$\nabla \cdot \left(\left(\frac{1}{2} \rho |\mathbf{v}|^2 + \rho \phi + \rho e + p \right) \mathbf{v} \right) = 0. \tag{5}$$

If heat transfer and work are considered, the equation (5) can be modified as equation (6) expressed as

$$\nabla \cdot \left(\left(\frac{1}{2} \rho |\mathbf{v}|^2 + \rho \phi + \rho e + p \right) \mathbf{v} \right) = Q - W, \tag{6}$$

where e is the total energy, $\mathbf{v}$ is the velocity, p is pressure and ρ is density of the fluid, $\frac{1}{2}\rho|\mathbf{v}|^2$ is the kinetic energy per unit volume of the fluid, $\rho\phi = \rho g z$: The potential energy per unit volume due to gravity (where z is the vertical coordinate in a gravitational field), ρe is the internal energy per unit volume.

Three primary components are present in all CFD codes. A pre-processor, which is used to input the problem geometry, generate the grid and also specify the flow parameter and boundary conditions for the code. A flow solver solves the flow's governing equations under the given conditions while a post-processor is used to manipulate the data and display the results in graphical and readable format.

2.3.2. Simulation software

ANSYS Fluent 2024R2, a versatile software for computational fluid dynamics (CFD) was used in this study to help comprehend radon distribution in indoor air. The software operates on the finite volume method (FVM) to break down the governing equations earlier defined and solve them through numerical techniques. This approach is especially effective for CFD as it accurately adheres to the continuity, momentum, and energy equations within every control volume or cell.

2.3.3. Geometric model

The model with an average dimension of 4.55 m × 4.55 m × 3.55 m along the x, y and z axes, respectively, with a window with a dimension of 0.8 m × 1.2 m (height × width) located at the center of the wall which faces the outdoor environment and the door with a dimension of 2.2 m × 1.0 m (height × width) directly facing the window as shown in Figure 1a. The surface area of the test room is 108.1 m^2 and its total volume is 74.126 m^3.

2.3.4. Meshing

One of the main factors influencing computation time in computationally demanding numerical simulations is the size of the computing grid. The ANSYS FLUENT program was used to mesh the numerical model (Figure 1b) using triangular unstructured grids with 8294 and 40688 elements and nodes, respectively.

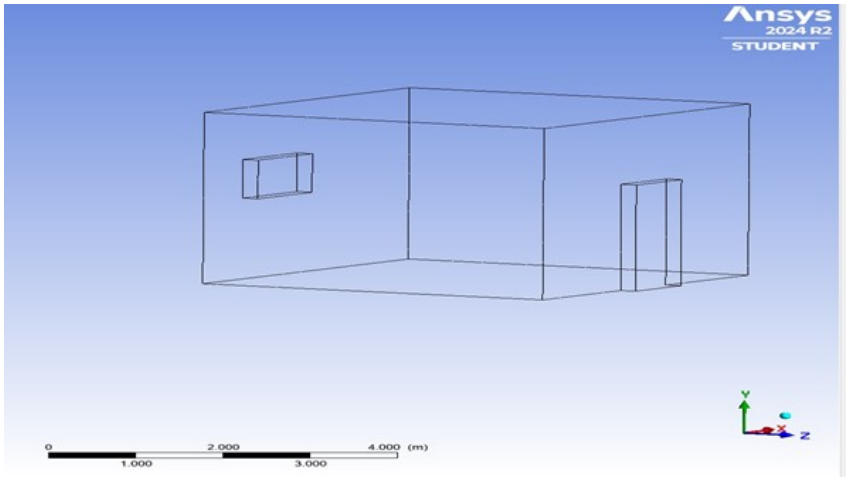

(a)

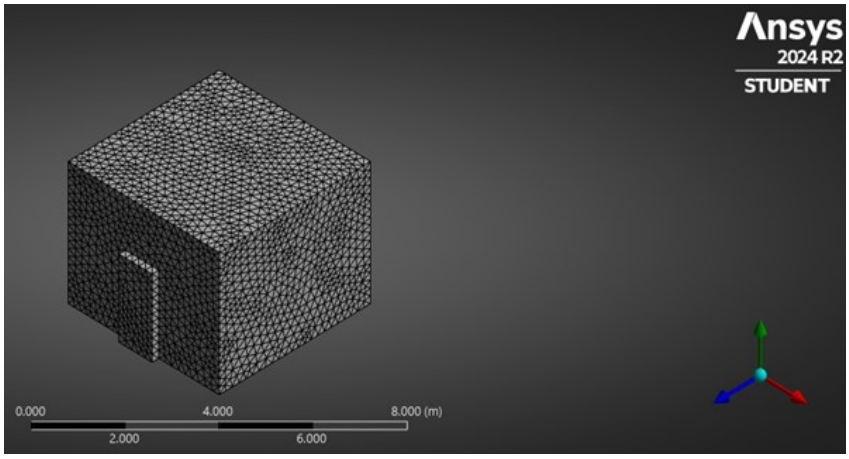

(b)

Figure 1: (a) Diagrammatic representation of the model room, (b) Meshing of the modelled room.

2.3.5. *Physical setting*

Ventilation was assumed to enter into the room via the window and departs through the door, temperature distribution inside the room was assumed to be homogeneous, materials used are air and radon as fluids, light concrete for the floor, dense concrete for the walls and roof.

2.3.6. *Solver*

Some assumptions considered in this study include standard k-epsilon, species transport, turbulence effect, incompressible air flow, steady-state indoor flow field and uniform indoor temperature distribution was used in the model. The standard k-ε model is a popular method for numerical simulation of room air flow [10]. Steady-state indoor flow was assumed because all conditions (pressure, density, temperature) does not change at any point with time.

Turbulence modeling. A ventilated space has turbulent air flows. In this work, turbulence modeling proved valid because of the high Reynolds number ($R_e > 2000$). For this study, the Standard k-ε model was used. The turbulent viscosity (μ_t) at each location and was related to local values of the turbulence kinetic energy, k, and the dissipation rate of turbulence energy, ε as:

$$\mu_t = \frac{C_\mu \rho k^2}{\varepsilon}, \tag{7}$$

where μ_t represent the turbulent viscosity, $C_\mu = 0.09$ which is an empirical constant and ρ is the fluid density. The following three-dimensional velocities were used to calculate the turbulent kinetic energy, k [17] expressed by equation (8).

$$k = \frac{1}{2}\left(\overline{u}^2 + \overline{v}^2 + \overline{w}^2\right). \tag{8}$$

Table 1: Boundary conditions for every surface of the room.

Surface	Boundary condition
Door	Outlet pressure
Window	Inlet velocity
Floor	No slip
Ceiling	No slip
Walls	No slip

Even when the ventilation rate is less than 0.2 m/s, air flow in a ventilated room typically exhibits a turbulence regime, necessitating the use of the turbulent k-ε model to solve the governing equations.

2.3.7. Domain properties

The room was modeled in 3-dimension and assumed to be stationary.

2.3.8. Boundary conditions

(a) Internal Surfaces

The internal walls, internal door and window were considered as wall with zero heat flux since indoor temperature is considered as uniform. Therefore, heat transfer through these surfaces were neglected.

(b) Inlet

Inlet boundary condition in the model were defined at the window which is the fresh air supplier, the defined specifications for this boundary were velocity magnitude and hydraulic diameter, turbulence specification which includes intermittency, turbulent intensity and species mass fraction (radon mass fraction). The boundary conditions of each surface of the room were stated in Table 1.

(c) Outlet

Outlet boundary condition was defined at the door, the air supply to the room from the window (inlet) exits the room via the door (outlet) that is the door is kept open. The air flow was considered to be incompressible inside the room and the flow rate was considered to be 1 since the flow field is a steady state flow fluid. Considering the outflow helps the model achieve quick convergence.

2.3.9. Solution

(a) Ventilation rate

The turbulence intensity and the velocity magnitude determine the ventilation rate. The velocity magnitude depends on the air change rate per hour, volume of the room and the ventilation area while turbulence intensity depends on the Reynold's number.

(b) Velocity magnitude

The inertial force is significantly greater than the viscous (shear) force in the vented room. The indoor airflows' Reynolds (Re) number is defined using [18]:

$$R_e = \frac{\rho \times V_{\text{vent}} \times Dh_{\text{vent}}}{\mu}, \tag{9}$$

where ρ represent air density, V_{vent} represent velocity, Dh_{vent} represent characteristic length of the air passage and μ is the air viscosity.

(c) Hydraulic diameter/ characteristic length

The hydraulic diameter of air passing through the inlet used for the simulation was obtained from equation (10) in order to compute the room's velocity inlet [18].

$$Dh_{\text{vent}} = \frac{4A}{P}, \tag{10}$$

where A is the area of the window and P is the wetted perimeter $2(L + B)$ of the window.

ASHRAE (2016) states that the range of air change rate per hour (ACH) for homes varies from 3 – 10 ACH. Therefore, the velocity of the vent was calculated using [18]:

$$V_{\text{vent}} = \frac{\text{ACH} \times V_{\text{room}}}{A_{\text{vent}}}, \tag{11}$$

where ACH is the Air Changes Per Hour, V_{room} is the volume of the room and A_{vent} is the ventilation area. The velocity at A_{vent} was computed at every change in air. The simulation took into account various air change rates between 2h^{-1} and 4h^{-1} ACH. The ACH was based on the amount of air circulation within each of the investigated rooms.

Table 2: Properties of fluids [11].

Property	Radon	Air
Density (kg/m^3)	9.73	1.225
Heat capacity (J kg^{-1} K^{-1})	93.55	1006.43
Thermal conductivity (W m^{-1} K^{-1})	0.0036	0.024
Viscosity (kg m^{-1} s^{-1})	2.445×10^{-5}	1.789×10^{-5}
Molecular weight (kg kmol^{-1})	222	28.966

Table 3: Properties of solids [11].

Property	Light concrete (floor)	Dense concrete (walls and roof)	Window	Door
Density (kg/m^3)	1200	2100	2700	720
Heat capacity (J kg^{-1} K^{-1})	1000	840	880	1250
Thermal conductivity (W m^{-1} K^{-1})	0.4	1.4	0.8	0.16

(d) Turbulence intensity

The measure of the fluctuations in fluid velocity within the turbulent flow was defined using the Reynold's number [19] expressed by:

$$I = 0.16(R_e)^{-1/8}. \tag{12}$$

The CFD code input parameter for radon generation rate can be calculated using [20]:

$$G_{\text{radon}}(\text{kg m}^{-3}\text{s}^{-1}) = \frac{\text{mass of radon}}{\text{volume of radon}}, \tag{13}$$

where mass of radon is expressed by equation (14):

$$\text{mass of radon}(\text{Bq s}^{-1}) = E \times \text{Area of the floor}. \tag{14}$$

2.3.10. Computational algorithm

(a) Material properties

The average radon concentration for each room was measured by RAD7 prior to being converted and entered into the CFD code. The fluid properties and the solid properties of the room were presented in Tables 2 and 3, respectively.

(b) Discretization method

Finite volume method was employed in the simulation because radon like many other substances is governed by the principle of conservation of mass. The finite volume method is designed to ensure local conservation of quantities such as radon concentration within each control volume, making it ideal for modeling transport phenomena including diffusion and advection which are central to radon movement in air, finite volume method can accurately model complex geometries and can also capture effectively the effects of obstacles like wall thus, making it accurate for simulating how radon concentration evolves in different parts of the room.

(c) Convergence monitoring values

Iteration: An iteration represents one complete cycle where the model is run using a specific set of inputs and a corresponding output is generated. The simulation repeats this process multiple times to obtain a range of results. Running multiple iterations helps to ensure that the results converge to a stable or predictable outcome. This is especially important in models where outputs might fluctuate in the early stages but stabilize over time. In some simulations, such as those involving probabilistic events, multiple iterations are needed to build a reliable statistical sample that accurately represents the system's behavior. Therefore 100 iterations were used in this study.

2.3.11. Post processor

This helps to extract useful information from the model, summarizing large volumes of data to make complex data easier to understand, visualizing reports that represents the simulation result in a comprehensible format. It also helps to identify trends anomalies or areas for further investigation.

2.3.12. Data analysis

The results obtained were subjected to statistical analysis using one-way analysis of variance at 0.05 level of significance. In addition, the measured and the simulated results were validated using metrics like root mean square error, coefficient of determination and percentage error.

Table 4: Statistical summary of the measured indoor radon concentration.

Room	N	Mean	Std. Deviation	Std. Error	95% Confidence Interval for Mean		Min	Max
					Lower Bound	Upper Bound		
1	3	44.7000	0.60828	0.35119	43.1890	46.2110	44.00	45.1
2	3	45.4000	0.36056	0.20817	44.5043	46.2957	45.00	45.7
3	3	45.3000	0.30000	0.17321	44.5548	46.0452	45.00	45.6
4	3	46.2000	0.17321	0.10000	45.7697	46.6303	46.00	46.3
5	3	43.6000	0.62450	0.36056	42.0487	45.1513	43.10	44.3
6	3	43.7000	0.55678	0.32146	42.3169	45.0831	43.20	44.3
7	3	46.6000	0.36056	0.20817	45.7043	47.4957	46.30	47
8	3	47.7000	0.26458	0.15275	47.0428	48.3572	47.50	48
9	3	50.2000	0.26458	0.15275	49.5428	50.8572	50.00	50.5
10	3	45.5667	0.37859	0.21858	44.6262	46.5071	45.30	46
Total	30	45.8967	1.92327	0.35114	45.1785	46.6148	43.10	50.5

Table 5: One sample statistic of the measured indoor radon concentration.

	Mean	Std. Deviation	T	Df	Sig. (2-tailed)	Mean Difference	95% Confidence Interval of the Difference	
							Lower	Upper
Radon	45.8967	1.92327	-154.08	29	0.000	-54.10333	-54.8215	-53.3852

Test Value = 100

Table 6: Validation of the measured and the simulated results.

Room	Measured (Bq/m^3)	Simulated (Bq/m^3)	RSME	R^2	%E
1	44.7	44.5	0.2	0.9669	0.447
2	45.4	45.1	0.3	0.4375	0.661
3	45.3	44.0	0.4	0.36	2.869
4	46.2	46.0	0.2	0.75	0.433
5	43.6	46.0	0.3	0.9815	0.6880
6	43.7	43.3	0.4	0.963	0.6860
7	46.6	46.3	0.3	0.8594	0.6465
8	47.7	47.4	0.3	0.9751	0.6280
9	50.2	50.0	0.2	0.9981	0.3984
10	45.5	45.2	0.3	1.0000	0.6590

RMSE - root mean square error, R^2 - coefficient of determination, %E - percentage error.

3. Results and discussion

3.1. Measurement result

The result obtained for the analysis of the measured indoor radon concentrations for each room investigated in the selected hostels were presented in Tables 4 and 5.

3.2. Simulation results

The results obtained for the air flow and radon concentration were presented in Figure 2-4 where the air velocity depends on the air change rate (ACH) and the radon concentration depends on the air velocity.

3.3. Performance evaluation

Table 6 present the results of the different performance metric applied in validating the accuracy of both the measured and the simulated radon distribution.

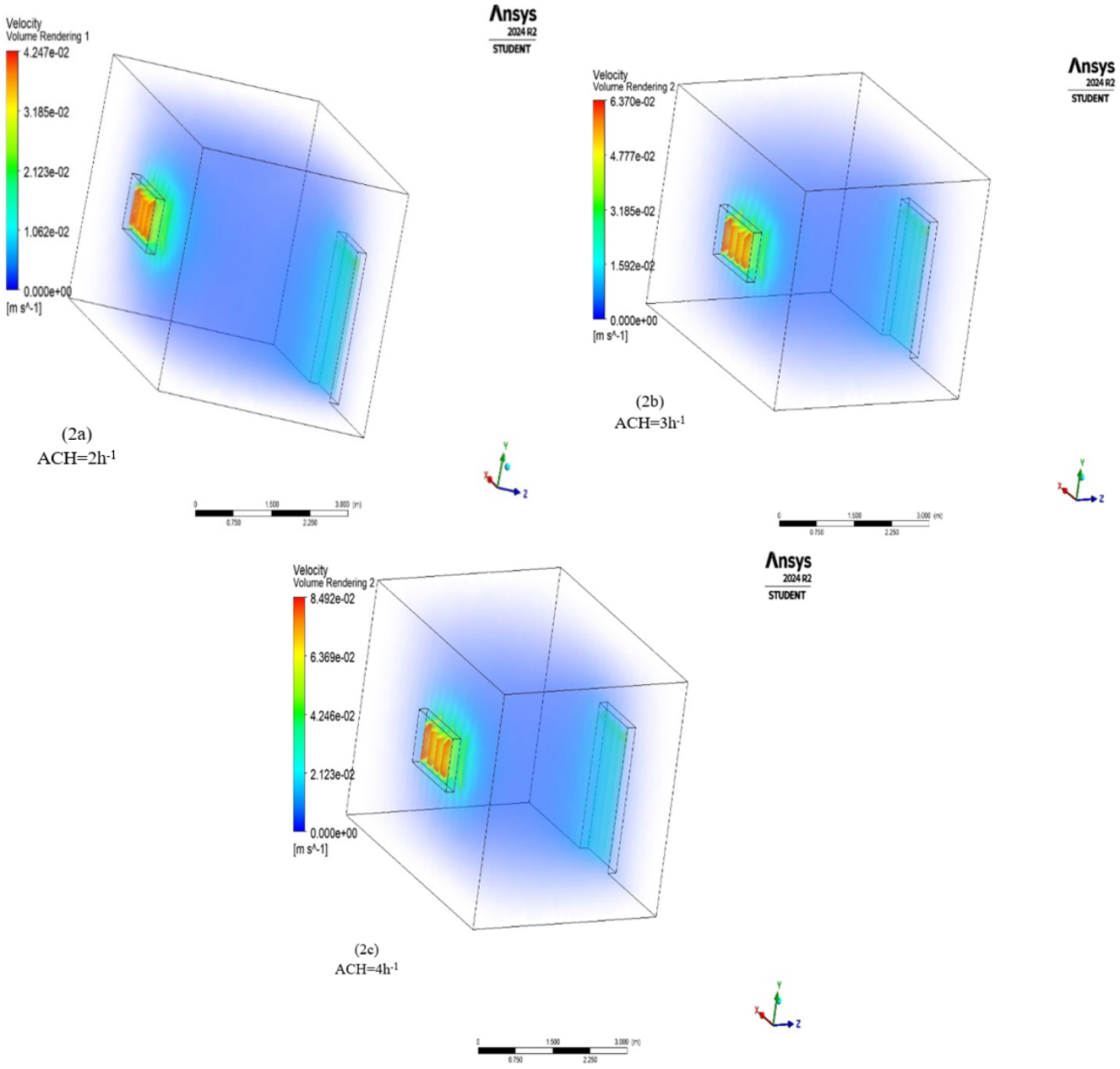

Figure 2: Velocity distribution at various ventilation rates in the test room model.

4. Discussion

Based on the results obtained (Table 4), the lowest radon concentration was found in hostel 5 with average value of 43.6 Bq/m^3 while the highest radon concentration recorded in hostel 9 is 50.2 Bq/m^3 which is below the action level (100 Bq/m^3) recommended by ICRP [21] and WHO [22], as well as 148 Bq/m^3 recommended by EPA [23]. The variation recorded in these buildings can be attributed to the geological features on which each building was sited, the building materials used in the construction, as well as the building age. This aligns with the report of Ref. [14] that geochemical and geological composition of the earth contribute significantly to the concentration of radionuclides in human's environment and also, the findings of Ref. [5] reporting that the lithology feature on which the buildings investigated in selected study locations of southwestern Nigeria influences the indoor radon concentration. In addition, Ref. [13] reported 17.17 Bq/m^3 and 16.90 Bq/m^3 in Ona Ara and Lagelu local government, respectively which is lower compared with 45.9 Bq/m^3 recorded in this study, according to Ref. [24] radon concentration were found to range from 64.9 Bq/m^3 to 94.7 Bq/m^3 in Daoudi and Hayy Al-Jamiaa, respectively, the variation could be as a result of the type of building material, age of the building, materials used in floor and walls, the presence of cracks or human activities. Comparing the obtained average radon with the world average value, we found that radon concentration in each room and the average radon concentration in all the rooms

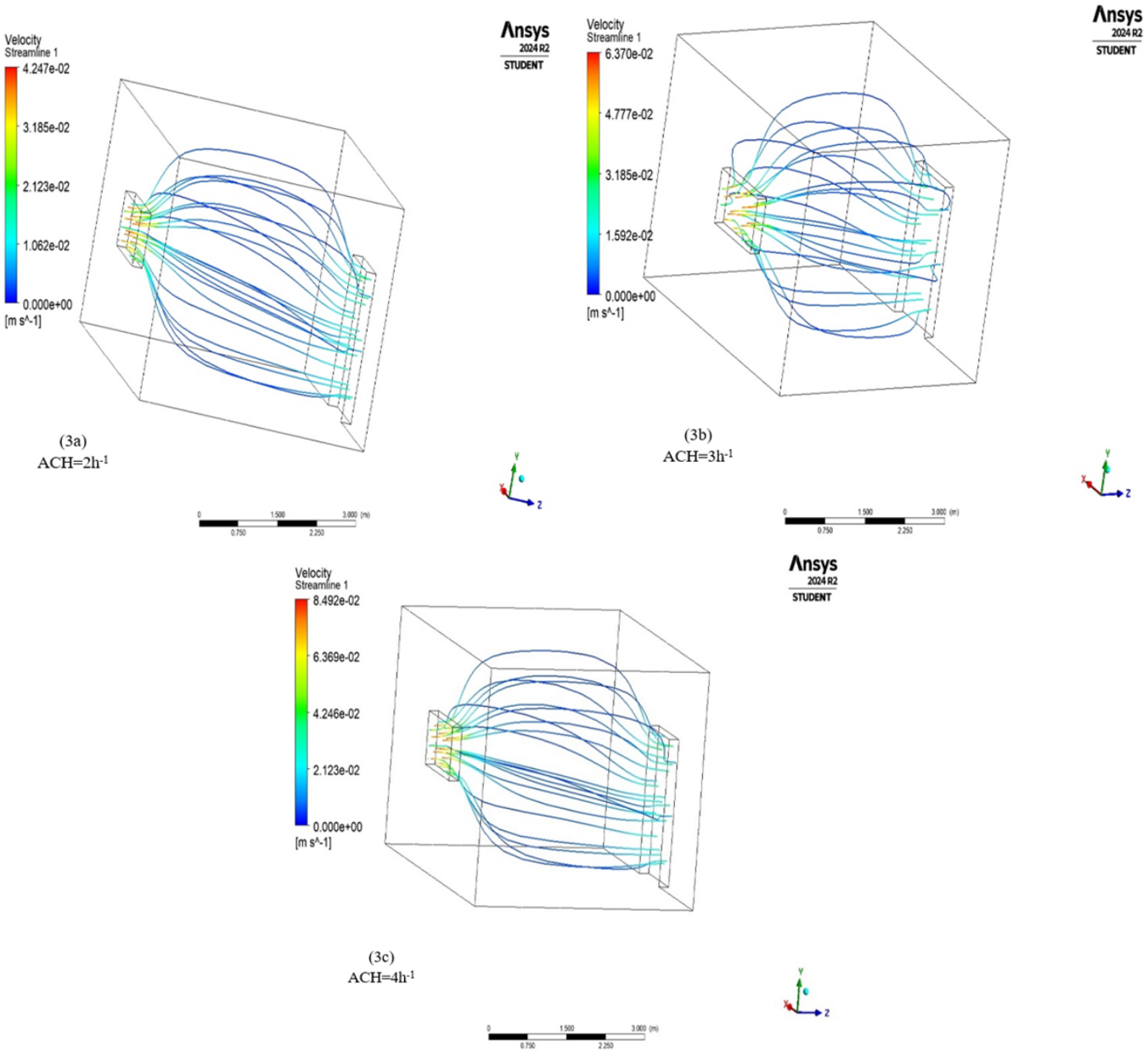

Figure 3: Velocity streamline at various ventilation rates in the test room model.

is higher than the world average value of 40 Bq/m^3 [13, 14, 25, 26] but below the international recommendation permissive level.

Descriptive statistics were computed to examine the average radon levels across varying numbers of rooms. The analysis included 30 observations, with 3 data points per room category (from 1 to 10 rooms). The overall mean radon level across all room categories was 45.90 (SD = 1.92), with a 95% confidence interval ranging from 45.18 to 46.61. Radon levels appeared to vary slightly in all the rooms, we observed the highest average radon level in room 9 (M = 50.20), followed by 8 rooms (M = 47.70) while the lowest average radon levels were found in room 5 (M = 43.60) and room 6 (M = 43.70). Standard deviations within each group were relatively small (ranging from 0.17 to 0.62), suggesting low variability within room categories. The range of radon levels across all groups spanned from a minimum of 43.10 to a maximum of 50.50.

A one-sample t-test (Table 5) was performed to assess whether the mean of radon significantly differed from a hypothesized value of 100 Bq/m^3, which is the recommended limit by WHO [22]. The analysis revealed a statistically significant difference between the sample mean and the test value, t (29) = -154.080, p ¡ .001. The sample mean (M ≈ 45.90) was significantly lower than 100, with a mean difference of -54.10 (95% CI [-54.82, -53.39]). These results strongly suggest that the true population mean of radon is significantly less than the test value.

From the average radon concentration, the annual absorbed dose and annual effective dose was calculated for each room and the

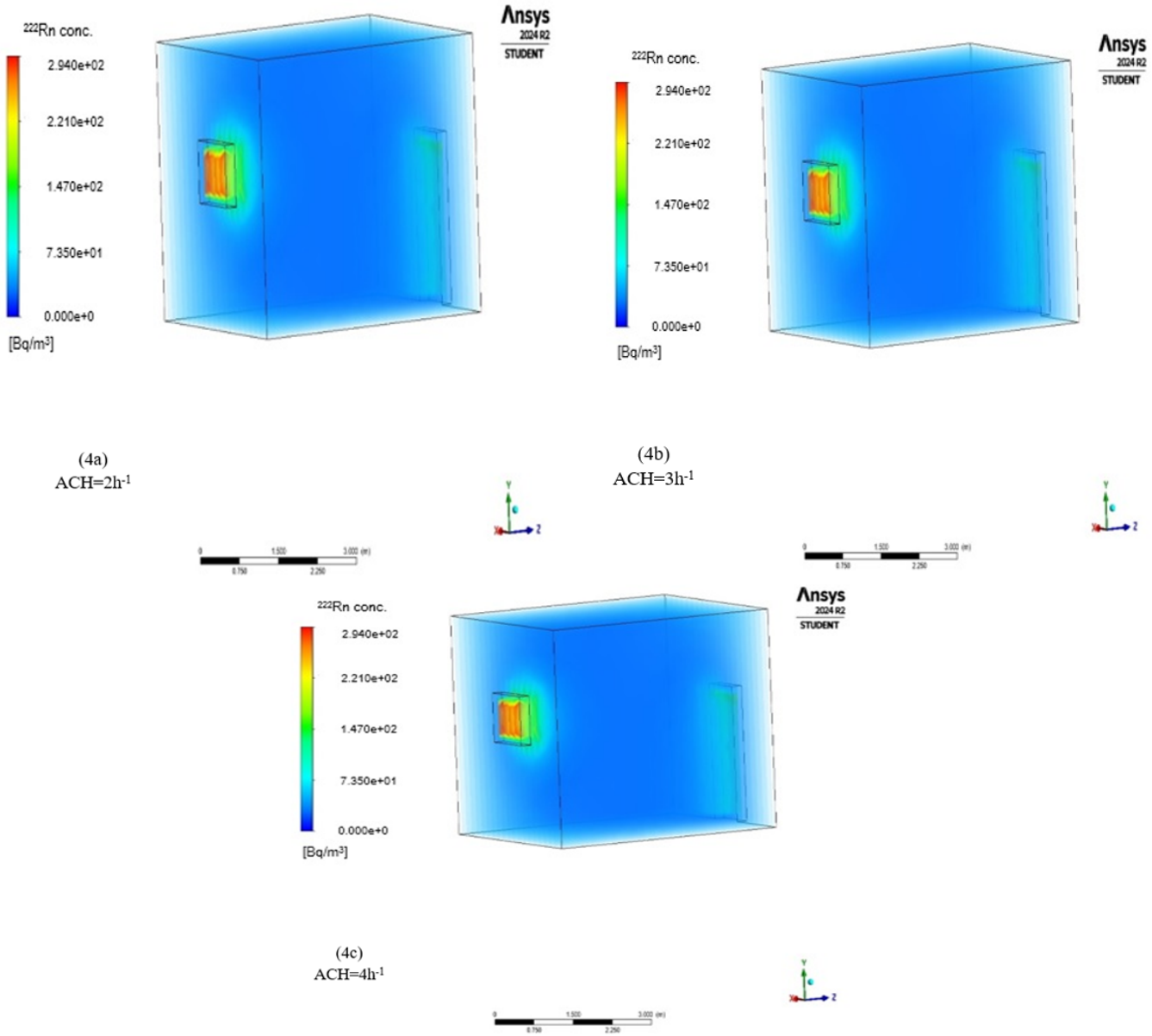

Figure 4: Radon concentration of 43.6 Bq/m^3 distribution at different ventilation rates in the test room model.

average annual absorbed dose was estimated to be 0.434 mSv/y. The room with the highest average concentration of radon indoors (room 9) also had effective dose to be the highest, all the rooms except room 5 and 6 exceeded the recommended limit of (1 mSv/y) the world average value for normal background radiation [13], the estimated average annual effective dose was 1.042 mSv/y, which is smaller than the range suggested by Ref. [20] of 3–10 mSv/y. With this, a prolong exposure to such amount of indoor radon could lead to detrimental health implications. This is because a lifetime of exposure to radon at 100 Bqm^{-3} increases the risk of lung cancer by 0.1% for non-smokers, and 2% for smokers according to ICRP [27]. In addition, findings revealed that radon and its decay products have been found to be responsible for 40 – 50% of total lifetime exposure of a person to health problems as reported [14] and that 3 – 14% of all lung cancers in a country result from exposure to radon gases, depending on the average radon level and the smoking prevalence in a country as reported by WHO [22]. In addition, report by Ref. [9] revealed that on the average, there is 0.2% to 0.6% of occurrence of lifetime cancer from chronic exposure to low-level radon gas using both the dosimetric and simulation technique. Although the occupancy rate in the investigated rooms is lower compare to that of the dwellings, thus it is very imperative that the student cultivate a healthy lifestyle of living so as to reduce the indoor radon level.

We observed in Figures 2 to 5 that as a result of the air flow velocities through the window (inlet), the radon gas concentration led towards the door (outlet). Radon was found to be concentrated at the inlet area, this could be as a result of the outdoor radon concentration, window wells, and proximity to radon sources, airflow and ventilation patterns. The ventilation profile revealed that

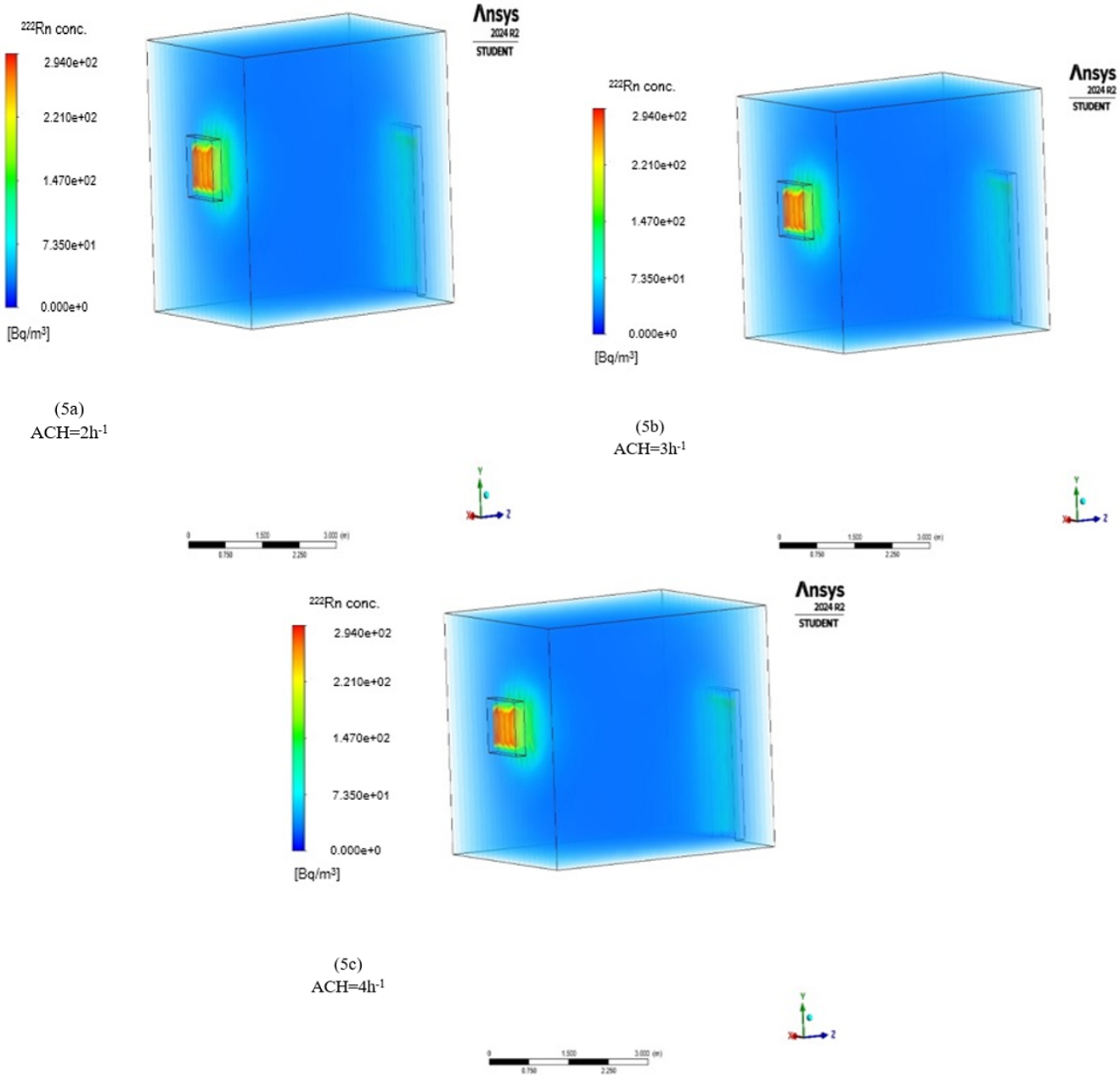

Figure 5: Radon concentration of 50.2 Bq/m^3 distribution at various ventilation rates in the test room model.

there was no significant difference in the radon concentration with different air flow rates used in this work. Concentration of radon at the center of the room according to the CFD simulation results was found to be very low. Figure 2 is the velocity volume rendering at different ventilation rate. Figure 3 shows the velocity streamlines in the test room model at various ventilation rate, Figure 4 and Figure 5 shows the concentration of radon in the modelled room with various ventilation rate. All this can be attributed to the boundary conditions such as steady state flow, no-slip conditions, and uniform indoor temperature defined during the simulation and which had little effect on the simulated results. This is because, all the rooms investigated practiced the same ventilation system by permitting the easy flow of external air into indoor air and at uniform room temperature.

In this study, the experimental result of the average indoor radon concentration was 45.89 Bq/m^3 and the corresponding annual effective dose was 1.042 mSv/yr. According to the simulation result, the average indoor radon concentration was 45.51 Bq/m^3 and from the inhalation of radon when ACH is 2 h^{-1}, 3 h^{-1} and 4 h^{-1}, the annual effective dose was calculated to be 1.03 mSv/y, these annual effective doses are less than the limit (3-10 mSv yr^{-1}) recommended by Ref. [21]. Based on Figure 3 and 4, the air flow pattern depends on the value of Reynold's number, the calculated Reynold's number for the room parameters and inlet velocity was found to be greater than 2000 which indicates turbulence flow. The simulated results for modelled rooms at different ventilation rate

corresponds well with the measured results and it followed the same pattern which was found to be below the limit (100 Bq/m^3) recommended by Ref. [22]. Ref. [11] assumed ACH=1 h^{-1} and the concentration of radon was simulated to be 49 Bq/m^3, higher radon concentration recorded could be as a result of lower ACH. Thus, the experiments provide room radon concentration values, while simulations display radon-air distribution, diffusion, and visualization, and provide possible lowest and highest concentrations in a room.

The comparison between measured and simulated radon concentrations across the ten studied rooms (Table 6) revealed a high level of agreement, suggesting the simulation model's robustness in replicating real-world radon exposure levels. The RMSE for all samples ranged from 0.2 to 0.4 indicating that the deviations between measured and modeled values were minimal and within acceptable margins for environmental radiation studies [14]. Furthermore, the R^2, which quantifies the strength of the linear relationship between the measured and simulated values, was above 0.85 in 9 out of the 10 locations, with several values nearing unity. This suggests a very strong positive correlation and confirms the accuracy and reliability of the simulation model. Notably, Room 10 achieved an R^2 of 1.000, representing a perfect fit between the model and observed data. The only significant deviation was observed in Sample 3, which had an R^2 of 0.36, potentially due to local environmental or measurement uncertainties not captured by the model [28]. The percentage error (%E) values were consistently low across all samples, ranging from 0.3984% to 2.869%, with an average error of less than 1%. This further demonstrates that the simulated values closely reflect the measured concentrations and supports the use of the model for predictive assessments in similar environmental settings. A percentage error below 10% is generally considered acceptable for indoor radon estimation models. These statistical indicators collectively validate the simulation approach adopted in this study, highlighting its potential for accurate prediction and mapping of indoor radon concentrations, especially in regions with limited measurement infrastructure.

5. Conclusion

In this study, the indoor radon concentration in students' residential hostels was measured and simulated using RAD7 and ANSYS Fluent 2024R2 simulation software, respectively. The results of radon concentration from the experimental measurement which ranges between 43.6 Bq/m^3 and 50.2 Bq/m^3 falls between 0 and 73.5 Bq/m^3 on the simulated results which shows agreement between the two methods. However, according to WHO there is no safe level to radon exposure but health risk increases significantly when levels exceed 100 Bq/m^3 and even at lower levels can contribute to an increased risk of lung cancer particularly for smokers. This study has revealed the impact of air velocity on indoor radon and also revealed the importance of numerical method (CFD) in the study of indoor radon concentration, radon-air distribution, diffusion and visualization which allow full control over the simulation environment and also variables such as indoor ventilation and diffusion coefficients can be adjusted to test different scenarios.

Data availability

Data will be made available upon reasonable request from the corresponding author.

Acknowledgment

The corresponding author acknowledges the Department of Pure and Applied Physics, Ladoke Akintola University of Technology software unit.

References

[1] M. A. Ashraf & M. M. Hanafiah, "Sustaining life on earth system through clean air, pure water and fertile soil", Environmental science and pollution research **26** (2019) 13679. https://doi.org/10.1007/s11356-018-3528-3.

[2] E. W. Pinchbeck, N. Szumilo, S. Roth & E. Vanino "The price of indoor air pollution: evidence from radon maps and the housing market", Journal of the Association of Environmental and Resource Economists **10** (2023) 1439. https://www.journals.uchicago.edu/doi/abs/10.1086/725028.

[3] E. A. Oni, O. O. Oladapo, M. K. Lawal, A. A. Aremu, P. S. Ayanlola, O. O. Oloyede & O. M. Oni "An overview of radon concentration in southwestern Nigeria", Physical Science and Biophysics Journal **6** (2022) 000220. https://doi.org/10.23880/psbj-16000220.

[4] K. Aladeniyi "Health risk evaluation of radon progeny exposure in Nigeria traditional mud houses", Journal of the Nigerian Society of Physical Sciences **6** (2024) 2128. https://doi.org/10.46481/jnsps.2024.2128.

[5] A. A. Aremu, M. O. Oni, O. O. Oladapo, E. A. Oni, P. S. Ayanlola, A. O. Adewoye, K. Amodu, M. K. Lawal & A. E. Oladipo. "Radiological risk assessment of radon inhalation in offices of selected institutions in southwestern Nigeria", LAUTECH Journal of Civil and Environmental Studies **11** (2023) 107. https://doi.org/10.36108/laujoces/3202.11.0101.

[6] M. Fuente, S. Long, D. Fenton, L. C. Hung, J. Goggins & M. Foleya "Review of recent radon research in Ireland, OPTI-SDS project and its impact on the National Radon Control Strategy", Applied radiation ad isotopes **163** (2020) 109210. https://doi.org/10.1016/j.apradiso.2020.109210.

[7] R. Rabi & L. Oufni "Study of radon dispersion in typical dwelling using CFD modeling combined with passive-active measurements", Radiation Physics and Chemistry **139** (2017) 40. http://dx.doi.org/10.1016/j.radphyschem.2017.04.012.

[8] S. Snehal & K. Priya "Review paper on air pollution monitoring system", International Journal of Advanced Research in Computer and Communication Engineering **4** (2015) 218. http://dx.doi.org/10.17148/IJARCCE.2015.4147.

[9] E. A. Oni, P. S. Ayanlola, A. A. Aremu, O. O. Oladapo & M. K. Lawal "Effect of chronic exposure to low-level radon gas from tertiary institutions workplaces in western Nigeria", Journal of Applied Science and Environmental Management **29** (2025) 831. https://dx.doi.org/10.4314/jasem.v29i3.19.
[10] A. Keramatollah, M. Jafar & M. Ghanbari "Simulation of ventilation effects on indoor radon". Management of Environmental Quality **24** (2013) 394. http://dx.doi.org/10.1108/14777831311322686.
[11] F. A. Lima, R. P. Palomino-Merino, V. M. Castano & G. Espinosa "Analysis of indoor radon distribution within a room by means of computational fluid dynamics (CFD) simulation", Journal of Nuclear Physics, Material Science Radiation and Applications **7** (2020) 89. http://dx.doi.org/10.15415/jnp.2020.72010.
[12] W. Y. A. Elola, T. L. Bambara, A. Doumounia, N. Kohio, S. Ouédraogo & F. Zougmore "Assessment of radon concentrations inside residential buildings and estimation of the dose in the city of Kaya, Burkina Faso", Open Journal of Applied Sciences **13** (2023) 1066. https://doi.org/10.4236/ojapps.2023.137085.
[13] M. R. Usikalu, V. Olatinwo, M. Akpochafor, M. A. Aweda, G. Giannini & V. Massimo "Measurement of radon concentration in selected houses in Ibadan, Nigeria," Journal of Physics: Conference Series **852** (2017) 012028. https://doi.org/10.1088/1742-6596/852/1/012028.
[14] United Nations Scientific Committee on the Effects of Atomic Radiation (UNSCEAR 2000). Sources and effects of ionizing radiation. Report to the General Assembly, with scientific annexes, Vol 1. [Online]. https://www.google.com/url?sa=t&source=web&rct=j&opi=89978449&url=https://www.unscear.org/unscear/uploads/documents/unscear-reports/UNSCEAR_2000_Report_Vol.I.pdf.
[15] R. Rabi, L. Oufni & H. Badry "Measurements and CFD modeling of outdoor radon dispersion", in 7th International Conference on Optimization and Applications, Wolfenbüttel, 1-7. 2021. https://doi.org/10.1109/icoa51614.2021.9442664.
[16] T. Wah-Yen, Y. Asako, N. A. Che sidik & G. Rui-Zher "Governing equations in CFD: derivation and a recent review", Journal of Progress in Energy and Environment **1** (2017) 1. ISSN: 2600-7762. [Online]. https://www.researchgate.net/publication/322031540_Governing_Equations_in_Computational_Fluid_Dynamics_Derivations_and_A_Recent_Review.
[17] A. Narkhede & N. Gnanasekaran "3D numerical modelling of turbulent flow in a channel partially filled with different blockage ratios of metal foam", Journal of Applied Fluid Mechanics **17** (2024) 548. https://doi.org/10.47176/jafm.17.3.2189.
[18] B. E. Anyaegbuna, A. O. Onokwai, N. T. Anyaegbuna, S. Iweriolor, I. D. Anyaegbuna, I. K. Adegun, O. S. Fayomi, D. E. Igbravwe & M. K. Onifade "Numerical analysis on mechanical ventilation impact on indoor air quality in a basement", Scientific Africa **25** (2024) 2468. https://doi.org/10.1016/j.sciaf.2024.e02310.
[19] E. C. Jung, G. H. Lee, E. B. Shim, H. Ha "Assessing the impact of turbulent kinetic energy boundary conditions on turbulent flow simulations using computational fluid dynamics", Scientific Reports **13** (2023) 14638. https://doi.org/10.1038/s41598-023-41324-w.
[20] M. Adelikhah, M. Imani & T. Kovacs "Measurements and computational fluid dynamics investigation of the indoor radon distribution in a typically natural ventilated room", Scientific reports **13** (2023) 2064. https://doi.org/10.1038/s41598-022-23642-7.
[21] International Commission on Radiation Protection (ICRP). Summary of ICRP recommendations on radon. ICRP ref. 4836-9756-8598. 2018. [Online]. https://www.icrpaedia.org/images/f/fd/ICRPRadonSummary.pdf.
[22] World health organization (WHO). Handbook on indoor radon: A public health perspective. WHO press, Switzerland. ISBN 978-92-4-156558-5. 2009. [Online]. https://iris.who.int/bitstream/handle/10665/44149/9789241547673_eng.pdf.
[23] US Environmental Protection Agency (EPA) EPA protocol for conducting radon and radon decay product measurements in multifamily buildings; Environmental Protection Agency: Washington. DC, 2017. [Online]. https://www.google.com/url?sa=t&source=web&rct=j&opi=89978449&url=https://nepis.epa.gov/Exe/ZyPURL.cgi%3FDockey%3D0000059B.TXT.
[24] S. A. Amin, S. D. Alalgawi & H. M. Hashim "Indoor radon concentrations and effective dose estimation in Al-Karkh side of Baghdad dwellings", Iranian Journal of Science & Technology **39** (2015) 491. https://doi.org/10.22099/ijsts.2015.3400.
[25] M. Fahiminia, F. R. Fouladi, R. Ardani, K. Naddafi, M. S. Hassanvand & B. A. Mohammad "Indoor radon measurements in residential dwellings in Qom, Iran", International Journal of Radiation Research **14** (2016) 331. http://dx.doi.org/10.18869/acadpub.ijrr.14.4.331.
[26] W. A. Alhamdi & K. M. S. Abdullah "Estimation of indoor radon concentration and dose evaluation of radon and its progeny in selected dwellings in Duhok city, Kurdistan Region, Iraq", International Journal of Radiation Research **20** (2022) 461. http://dx.doi.org/10.52547/ijrr.20.2.30.
[27] M. Tirmarche, J. D. Harrison, D. Laurier, F. Paquet, E. Blanchardon & J. W. Marsh, "International Commission on Radiological Protection. ICRP Publication 115. Lung cancer risk from radon and progeny and statement on radon", Annals of the ICRP **40** (2010) 1. https://doi.org/10.1016/j.icrp.2011.08.011.
[28] U.S. Environmental Protection Agency. (2009). A citizen's guide to radon: the guide to protecting yourself and your family from radon. Washington, DC: U.S. EPA. https://www.epa.gov/radon.